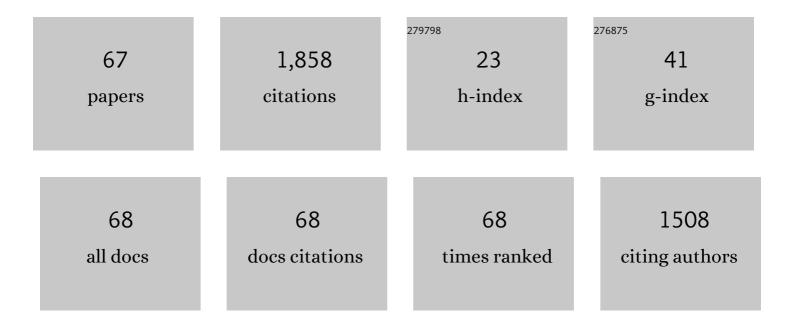
List of Publications by Year in descending order

Source: https://exaly.com/author-pdf/3811361/publications.pdf Version: 2024-02-01



#	Article	IF	CITATIONS
1	Double-perovskites A2FeMoO6â^' (A= Ca, Sr, Ba) as anodes for solid oxide fuel cells. Journal of Power Sources, 2010, 195, 6356-6366.	7.8	166
2	SmBaCo2O5+x double-perovskite structure cathode material for intermediate-temperature solid-oxide fuel cells. Journal of Power Sources, 2008, 185, 754-758.	7.8	155
3	Performances of LnBaCo2O5+x–Ce0.8Sm0.2O1.9 composite cathodes for intermediate-temperature solid oxide fuel cells. Journal of Power Sources, 2010, 195, 2174-2181.	7.8	143
4	Novel SrCo1â^'yNbyO3â^'δ cathodes for intermediate-temperature solid oxide fuel cells. Journal of Power Sources, 2010, 195, 3772-3778.	7.8	134
5	La0.6Sr0.4Fe0.8Cu0.2O3â^' perovskite oxide as cathode for IT-SOFC. International Journal of Hydrogen Energy, 2012, 37, 11963-11968.	7.1	93
6	Electrochemical performances of LaBaCuFeO5+x and LaBaCuCoO5+x as potential cathode materials for intermediate-temperature solid oxide fuel cells. Electrochemistry Communications, 2009, 11, 80-83.	4.7	72
7	Cobalt-free cathode material SrFe0.9Nb0.1O3â^ for intermediate-temperature solid oxide fuel cells. Electrochemistry Communications, 2010, 12, 285-287.	4.7	67
8	Synthesis of Zn2SnO4 via a co-precipitation method and its gas-sensing property toward ethanol. Sensors and Actuators B: Chemical, 2015, 213, 155-163.	7.8	62
9	La0.7Ca0.3CrO3–Ce0.8Gd0.2O1.9 composites as symmetrical electrodes for solid-oxide fuel cells. Journal of Power Sources, 2011, 196, 76-83.	7.8	52
10	Preparation and characterization of cellulose nanofibers from partly mercerized cotton by mixed acid hydrolysis. Cellulose, 2014, 21, 301-309.	4.9	52
11	Layered Perovskite GdBaCuCoO[sub 5+Î] Cathode Material for Intermediate-Temperature Solid Oxide Fuel Cells. Journal of the Electrochemical Society, 2010, 157, B628.	2.9	39
12	Reversible regulation of upconversion luminescence in new photochromic ferroelectric materials: Bi _{4â^*x} Er _x Ti ₃ O ₁₂ ceramics. Inorganic Chemistry Frontiers, 2019, 6, 2756-2766.	6.0	34
13	Preparation and electrochemical properties of La1.5Pr0.5NiO4 and La1.5Pr0.5Ni0.9Cu0.1O4 cathode materials for intermediate-temperature solid oxide fuel cells. Materials Research Bulletin, 2019, 113, 25-30.	5.2	34
14	Evaluation of double perovskite Sr2FeTiO6â~δas potential cathode or anode materials for intermediate-temperature solid oxide fuel cells. Ceramics International, 2015, 41, 12393-12400.	4.8	33
15	Combustion synthesis and properties of highly phase-pure perovskite electrolyte Co-doped La0.9Sr0.1Ga0.8Mg0.2O2.85 for IT-SOFCs. International Journal of Hydrogen Energy, 2010, 35, 294-300.	7.1	32
16	Synthesis and characterization of BaBi0.05Co0.8Nb0.15O3â~δas a potential IT-SOFCs cathode material. Journal of Alloys and Compounds, 2015, 627, 320-323.	5.5	31
17	Template-free hydrothermal synthesis of ZnO micro/nano-materials and their application in acetone sensing properties. Superlattices and Microstructures, 2015, 77, 1-11.	3.1	29
18	Evaluation and optimization of SrCo0.9Ta0.1O3â^'î´ perovskite as cathode for solid oxide fuel cells. Current Applied Physics, 2012, 12, 1092-1095.	2.4	27

#	Article	IF	CITATIONS
19	High performance temperature sensing and optical heating of Tm3+- and Yb3+- codoped SrBi4Ti4O15 up-conversion luminescence nanoparticles. Ceramics International, 2019, 45, 18084-18090.	4.8	26
20	An engineering ceramic-used high-temperature-resistant inorganic phosphate-based adhesive self-reinforced by in-situ growth of mullite whiskers. Journal of the European Ceramic Society, 2019, 39, 1703-1706.	5.7	26
21	Ba0.9Sr0.1Co0.9In0.1O3â^' perovskite as cathode material for IT-SOFC. Journal of Alloys and Compounds, 2015, 641, 234-237.	5.5	24
22	Novel cobalt-free cathode material (Nd0.9La0.1)2(Ni0.74Cu0.21Al0.05)O4+δ for intermediate-temperature solid oxide fuel cells. Ceramics International, 2015, 41, 639-643.	4.8	23
23	Electrode properties of (Pr0.9La0.1)2â^'x(Ni0.74Cu0.21Al0.05)O4+Î′ (with x=0, 0.05, and 0.1) as cathodes in IT-SOFCs. Journal of Alloys and Compounds, 2019, 793, 519-525.	5.5	23
24	Highly sensitive up-conversion thermometric performance in Nd3+ and Yb3+ sensitized Ba4La2Ti4Nb6O30 based on near-infrared emissions. Journal of Physics and Chemistry of Solids, 2019, 124, 130-136.	4.0	23
25	Effect of Al:P ratio on bonding performance of high-temperature resistant aluminum phosphate adhesive. International Journal of Adhesion and Adhesives, 2020, 100, 102627.	2.9	23
26	A new class of upconversion luminescence tuning materials based on non-photochromic reaction: Er3+-activated Ba0.7Sr0.3Nb2O6 ferroelectrics. Acta Materialia, 2021, 205, 116557.	7.9	22
27	Electrode properties of a spinel family, AFe2O4 (A = Co, Ni, Cu), as new cathode for solid oxide fuel cells. Journal of Materials Science: Materials in Electronics, 2019, 30, 5573-5579.	2.2	21
28	LaSrMnCoO5+l̂´ as cathode for intermediate-temperature solid oxide fuel cells. Electrochemistry Communications, 2012, 19, 36-38.	4.7	20
29	LaBaCuFeO5+Î`–Ce0.8Sm0.2O1.9 as composite cathode for solid oxide fuel cells. Ceramics International, 2012, 38, 1529-1532.	4.8	20
30	Bonding performance and mechanism of a heat-resistant composite precursor adhesive (RT-1000â ^{~~} C) for TC4 titanium alloy. Journal of Micromechanics and Molecular Physics, 2020, 05, 2050016.	1.2	19
31	Ultrasound-assisted synthesis of CuO nanostructures templated by cotton fibers. Materials Research Bulletin, 2012, 47, 3135-3140.	5.2	17
32	Evaluation of GdBaCuCo0.5Fe0.5O5+ as cathode material for intermediate temperature solid oxide fuel cells. Ceramics International, 2012, 38, 2899-2903.	4.8	17
33	Highly selective n-butanol gas sensor based on porous In2O3 nanoparticles prepared by solvothermal treatment. Materials Science in Semiconductor Processing, 2018, 83, 139-143.	4.0	17
34	Investigation of cobalt-free perovskite Sr2FeTi0.75Mo0.25O6â^Î^ as new cathode for solid oxide fuel cells. Materials Research Bulletin, 2016, 74, 129-133.	5.2	16
35	Optical multi-functionalities of Er3+- and Yb3+-sensitized strontium bismuth titanate nanoparticles. Journal of Alloys and Compounds, 2019, 801, 1-9.	5.5	16
36	Mullite whiskers grown in situ reinforce a pre-ceramic resin adhesive for silicon carbide ceramics. Ceramics International, 2019, 45, 11131-11135.	4.8	16

#	Article	IF	CITATIONS
37	Synthesis of Sm doped SnO2 nanoparticles and their ethanol gas traces detection. Ceramics International, 2021, 47, 26501-26510.	4.8	15
38	Chromium carbide micro-whiskers: Preparation and strengthening effects in extreme conditions with experiments and molecular dynamics simulations. Journal of Solid State Chemistry, 2020, 291, 121598.	2.9	14
39	Assessment of Nd1.5Pr0.5Ni1â``xMxO4+δ (M = Cu, Co, Mo; x = 0, 0.05 and 0.1) as cathode mar intermediate-temperature solid oxide fuel cell. Journal of Materials Science: Materials in Electronics, 2020, 31, 949-958.	terials for 2.2	12
40	Advanced high-temperature resistant (RT-1000°C) aluminum phosphate-based adhesive for titanium superalloys in extreme environments. Ceramics International, 2021, 47, 32988-33001.	4.8	12
41	Investigation of antibacterial properties of nano-ZnO assembled cotton fibers. Fibers and Polymers, 2013, 14, 990-995.	2.1	11
42	Novel YBaCo3.2Ga0.807+l̂´as a cathode material and performance optimization for IT-SOFCs. International Journal of Hydrogen Energy, 2014, 39, 10710-10717.	7.1	11
43	A heat-resistant glass-modified multi-component phosphate adhesive for repair and connection of superalloy in extreme environment. Journal of Alloys and Compounds, 2018, 745, 868-873.	5.5	11
44	Analysis of the upconversion photoluminescence spectra as a probe of local microstructure in Y ₂ O ₃ /Eu ³⁺ nanotubes under high pressure. RSC Advances, 2015, 5, 3130-3134.	3.6	10
45	Preparation and electrochemical properties of an La-doped Pr2Ni0.85Cu0.1Al0.05O4+δ cathode material for an IT-SOFC. Journal of Alloys and Compounds, 2020, 824, 153967.	5.5	10
46	Novel BaBi 0.05 Co 0.8 Ta 0.15 O 3â^îŕ cathode material for intermediate temperature solid oxide fuel cells. Materials Letters, 2017, 193, 105-107.	2.6	9
47	A chiral open-framework fluorinated cobalt phosphate consists of distorted F-encapsulated double 4-ring units with bulk homochirality. Chemical Communications, 2019, 55, 226-228.	4.1	9
48	Well-aligned periodic germanium nanoisland arrays with large areas and improved field emission performance induced by femtosecond laser. Applied Surface Science, 2020, 508, 145308.	6.1	9
49	Electrochemical characterization of LaBaCuCoO5+̴–Sm0.2Ce0.8O1.9 composite cathode for intermediate-temperature solid oxide fuel cells. Materials Research Bulletin, 2012, 47, 101-105.	5.2	8
50	Cobalt-free quintuple perovskite Sm 1.875 Ba 3.125 Fe 5 O 15â^î´ as a novel cathode for intermediate temperature solid oxide fuel cells. Ceramics International, 2016, 42, 10469-10471.	4.8	8
51	Phase stability and electrochemical performance of Y0.5Ca0.5â^'xInxBaCo3.2Ga0.8O7+Î′ (xÂ=Â0 and 0.1) as cathodes for intermediate temperature solid oxide fuel cells. Journal of Alloys and Compounds, 2016, 680, 163-168.	5.5	8
52	Up-conversion luminescence regulation and its boosting by polarization in Er3+/Yb3+ doped SrBi8Ti7O27 photochromic ceramics for optical switching application. Journal of Alloys and Compounds, 2021, 883, 161024.	5.5	8
53	Preparation, characterization, and electrochemical properties of YBaCo3.4Al0.3Ga0.3O7+δ and YBaCo3.2Al0.4Ga0.4O7+δ cathodes for IT-SOFCs. Ceramics International, 2014, 40, 13481-13485.	4.8	7
54	Vibrational Properties and Polymerization of Corannulene under Pressure, Probed by Raman and Infrared Spectroscopies. Journal of Physical Chemistry C, 2019, 123, 23674-23681.	3.1	7

#	Article	IF	CITATIONS
55	CO2-tolerant Sr2CoTaO6- \hat{l}' double perovskite oxide as a novel cathode for intermediate-temperature solid oxide fuel cell. Materials Research Bulletin, 2022, 146, 111624.	5.2	7
56	A novel heat-resistant resin-based adhesive for high-temperature alloy connection and repair. Journal of Alloys and Compounds, 2019, 774, 46-51.	5.5	6
57	Pressure-induced structural transitions and metallization in hollow ZnMn2O4 microspheres. Journal of Alloys and Compounds, 2020, 818, 152881.	5.5	6
58	Electrochemical properties of La1.5Pr0.5Ni0.95â^Cu Al0.05O4+ Ruddlesden-Popper phase as cathodes for intermediate-temperature solid oxide fuel cells. Materials Research Bulletin, 2020, 131, 110986.	5.2	6
59	Study of synthesis and photocatalytic performance of the monoclinic/cubic heterophase junction of rare earth doped zirconia. Journal of Physics and Chemistry of Solids, 2021, 159, 110286.	4.0	6
60	The pressure induced amorphization and behavior of octahedron in Y ₂ O ₃ /Eu ³⁺ nanotubes. Materials Research Express, 2014, 1, 025013.	1.6	5
61	Investigation of the lattice behavior of cubic Y ₂ O ₃ /Eu ³⁺ nanotubes under high pressure. Physica Status Solidi (B): Basic Research, 2016, 253, 2204-2208.	1.5	3
62	PrSr3Fe3O10â^²Î´ as cobalt-free cathode for intermediate-temperature solid oxide fuel cell. Materials Letters, 2020, 279, 128489.	2.6	3
63	Chromium carbide micro-whiskers dataset: Morphologies with scanning and transmission electronic microscopy. Data in Brief, 2020, 32, 106222.	1.0	3
64	High Pressure and High Temperature Induced Polymerization of C ₆₀ Solvates: The Effect of Intercalated Aromatic Solvents. Journal of Physical Chemistry C, 2021, 125, 17155-17163.	3.1	3
65	Shape-diversified silver nanostructures on Al foil fabricated in micellar template for high performance surface enhanced Raman scattering applications. Optical Materials, 2021, 121, 111629.	3.6	3
66	Comparative studies of BaBi0.05Zr0.1Co0.85â^`xNbxO3â^`δ (x = 0 and 0.05) as cathodes for intermediate-temperature solid oxide fuel cells. Journal of Materials Science: Materials in Electronics, 2020, 31, 11819-11824.	2.2	2
67	GeSn/GeSiSn double-heterojunction short channel tunnel field-effect transistor design. Japanese Journal of Applied Physics, 2020, 59, 034001.	1.5	1